Ministry of Science, Research and Technology
University of Bonab

Mechanics in Nano-Engineering

journal homepage: https://mneng.ubonab.ac.ir/

Mechanics in NANO-ENGINEERING

Numerical Investigation of Viscous Dissipation Effects on Mixed Convection of a Water-Based TiO_2 Nanofluid in a Lid-Driven Cavity with an Aspect Ratio of L/H = 4

Seyed Hamed Adibi [a,b]

a Department of Mechanical Engineering, University of Tabriz, Tabriz, Iran
[b] Power Generation Management Company (Tabriz Thermal Power Plant)

ARTICLE INFO

Article history:
Received 9 12 2026
Received in revised form 11 1 2026
Accepted 11 8 2026

Keywords:
Mixed convection;
Lid-driven cavity;
TiO_2 nanofluid;
Viscous dissipation;
Eckert number;
Finite volume method

ABSTRACT

This study numerically investigates mixed convection in a rectangular cavity filled with a water-based titanium dioxide TiO2 nanofluid, focusing on the influence of viscous dissipation on the flow and temperature fields. The cavity has an aspect ratio of 4, with its upper and lower walls moving in opposite directions at equal dimensionless velocities. The vertical sidewalls are stationary and thermally insulated. The governing equations are solved using the finite volume method, with the Reynolds, Grashof, and Prandtl numbers fixed at 49, 16, and 6, respectively, corresponding to a Richardson number of $Ri = Gr/Re^2 \approx 0.0067$, i.e., a forced-convection-dominated regime with a weak buoyancy contribution and the nanoparticle volume fraction maintained at 0.03. The Eckert number is varied from 0.0 to 0.3 to examine the contribution of viscous dissipation to the thermal behavior. Numerical convergence, grid independence, and validation against previously published skin-friction data are considered to assess the numerical results. The results show that the streamline patterns and velocity profiles remain qualitatively similar across the investigated Eckert numbers, indicating a limited influence of viscous dissipation on the overall flow structure. In contrast, the temperature profiles exhibit noticeable changes as the Eckert number increases. The dimensionless temperature generally rises over a substantial portion of the cavity, demonstrating the importance of viscous heating in the energy balance. These findings indicate that viscous dissipation affects the thermal field more strongly than the overall velocity distribution under the present operating conditions.

1. Introduction

Mixed convection in lid-driven cavities has attracted considerable attention because it involves the interaction of shear-driven flow generated by moving walls and buoyancy-driven motion induced by temperature differences. This type of flow is relevant to various engineering applications, including electronic cooling, heat exchangers, thermal management systems, and energy conversion devices. The resulting flow structure and heat transfer characteristics depend on several parameters,

particularly the Reynolds, Grashof, and Prandtl numbers, as well as the cavity geometry and thermal boundary conditions. Ghia et al. [1] established an important numerical benchmark for incompressible flow in a lid-driven cavity, providing a basis for the verification of computational fluid dynamics methods. Subsequently, Iwatsu et al. [2] investigated mixed convection in a driven cavity subjected to a stable vertical temperature gradient, demonstrating the importance of the interaction between wall-driven motion and thermal buoyancy.

The use of nanofluids has introduced an additional approach to modifying the thermal characteristics of conventional heat-transfer fluids. Nanofluids consist of a base fluid containing dispersed nanoparticles, which can alter the effective thermophysical properties of the resulting suspension. Choi and Eastman [3] introduced the concept of enhancing the thermal conductivity of conventional fluids through the addition of nanoparticles. Since then, numerous numerical and experimental investigations have examined the thermal behavior of nanofluids in different flow configurations. Chamkha and Abu-Nada [4] numerically studied mixed convection in single- and double-lid-driven cavities filled with water–Al_2O_3 nanofluid and demonstrated that the predicted heat-transfer performance depends on both the nanoparticle concentration and the viscosity model. Alinia et al. [5] investigated mixed convection in an inclined two-sided lid-driven cavity containing a water-based nanofluid, considering the effects of inclination angle, Richardson number, and nanoparticle volume fraction. Their work highlighted the influence of buoyancy and cavity orientation on the resulting thermal field.

Further studies have considered more complex cavity configurations and different numerical approaches. Chatterjee et al. [6] investigated mixed convection of a Cu–water nanofluid in a lid-driven cavity containing a rotating circular cylinder, showing that the flow and heat transfer depend on the rotational speed and the strength of mixed convection. Sheremet and Pop [7] examined mixed convection in a lid-driven cavity using Buongiorno's mathematical model, incorporating nanoparticle transport mechanisms into the governing equations. Rahmati et al. [8] employed the lattice Boltzmann method to investigate mixed convection in a double-lid-driven cavity filled with Cu–water nanofluid. Their results demonstrated that the thermal boundary conditions and the relative importance of forced and natural convection can influence the flow patterns and heat-transfer characteristics. Similarly, Jmai et al. [9] investigated mixed convection in a two-sided lid-driven cavity partially heated and filled with nanofluid, emphasizing the roles of wall-speed ratio and buoyancy effects.

The broader literature on nanofluid convection in enclosures has been reviewed by Hemmat Esfe et al. [10] and Izadi et al. [11]. These reviews summarize the effects of cavity geometry, boundary

conditions, nanoparticle concentration, and governing dimensionless parameters on fluid flow and heat transfer. Boulahia et al. [12] further investigated mixed convection in a two-sided lid-driven cavity containing nanofluids and triangular heat sources, considering different nanoparticle materials, particle sizes, and Richardson numbers. Adibi et al. [13] examined forced, natural, and mixed convection involving water-based nanofluids containing different ceramic nanoparticles, including TiO_2. Their study demonstrated the applicability of numerical methods to the investigation of flow and heat transfer in different cavity configurations and provided relevant reference data for evaluating numerical predictions. More recently, Keklikcioğlu Çakmak et al. [14] investigated mixed convection in a lid-driven cavity filled with Al_2O_3–water nanofluid using a finite volume formulation, further illustrating the continuing interest in numerical modeling of nanofluid-filled enclosures.

In addition to nanoparticle properties and buoyancy effects, viscous dissipation can influence the energy balance when mechanical energy is converted into thermal energy through viscous stresses. The relative importance of this mechanism is characterized by the Eckert number, (Ec). Aydin and Kaya [15] studied mixed convection of a viscous-dissipating fluid along a vertical flat plate under aiding and opposing buoyancy conditions. Their results demonstrated that the influence of viscous dissipation on temperature and heat transfer depends on the governing parameters and the physical configuration. Viscous dissipation has also been considered in more recent cavity-flow studies, including investigations of mixed convection in nonrectangular enclosures. Such studies indicate that the thermal response to increasing the Eckert number can be significant even when the overall flow structure remains comparatively stable.

Despite the extensive literature on mixed convection in lid-driven cavities and the thermal behavior of nanofluids, the influence of viscous dissipation remains dependent on the specific combination of geometry, wall motion, and thermal boundary conditions. In particular, the interaction between opposing horizontal wall motions, a substantial cavity aspect ratio, and a fixed nanoparticle concentration provides a configuration for which the relative responses of the velocity and temperature fields deserve further examination. The present study addresses this issue by numerically investigating mixed convection in a rectangular cavity with an aspect ratio of (L/H=4), filled with a water-based TiO_2 nanofluid at a nanoparticle volume fraction of 0.03. The upper and lower walls move in opposite directions with equal dimensionless velocities and are maintained at dimensionless temperatures of (-1) and (+1), respectively, while the stationary vertical walls are thermally insulated.

The Reynolds, Grashof, and Prandtl numbers are fixed at (Re=49), (Gr=16), and (Pr=6), respectively, while the Eckert number is varied from 0.0 to 0.3. The governing equations are discretized using the finite volume method. The numerical solution is assessed through convergence analysis, a grid-independence study, and comparison with previously published skin-friction data. The effects of the Eckert number are then examined using streamline patterns and horizontal and vertical velocity and temperature profiles. The main objective is to determine whether viscous dissipation produces noticeable changes in the flow structure and velocity distribution or primarily modifies the temperature field under the specified conditions.

2. Methods and Material

2.1. Physical Model and Boundary Conditions

The present study investigates mixed convection and fluid flow in a two-dimensional rectangular cavity filled with a water-based titanium dioxide TiO_2 nanofluid. The cavity has an aspect ratio of (L/H=4), where (L) and (H) denote the cavity length and height, respectively. The upper and lower horizontal walls move in opposite directions with equal dimensionless velocities, while the vertical sidewalls remain stationary. In addition to the shear-driven flow induced by the moving walls, the temperature difference between the horizontal boundaries generates buoyancy forces within the cavity.

The upper wall moves to the left with a dimensionless velocity of (u=-1) and is maintained at a dimensionless temperature of (T=-1). Conversely, the lower wall moves to the right with a dimensionless velocity of (u=1) and is maintained at (T=1). Both vertical sidewalls are stationary and thermally insulated. The corresponding boundary conditions are Shown in Figure 1.

The nanoparticle volume fraction is fixed at (C=0.03), corresponding to a 3% volume concentration of (TiO_2) nanoparticles. The effects of viscous dissipation are investigated by varying the Eckert number while maintaining the Reynolds, Grashof, and Prandtl numbers at (Re=49), (Gr=16), and (Pr=6), respectively. This approach allows the influence of viscous dissipation on the velocity and temperature fields to be examined under otherwise identical flow conditions.

The selected Reynolds and Grashof numbers (Re = 49, Gr = 16) yield a Richardson number of $Ri = Gr/Re^2 \approx 0.0067$, indicating that the flow is dominated by the shear-driven motion of the walls, with buoyancy playing a secondary role. These values were chosen deliberately to distinguish the present configuration from standard lid-driven cavity benchmarks (typically Re = 100–1000) and to provide a parameter regime in which the influence of viscous dissipation can be examined under a stable, forced-convection-dominated flow.

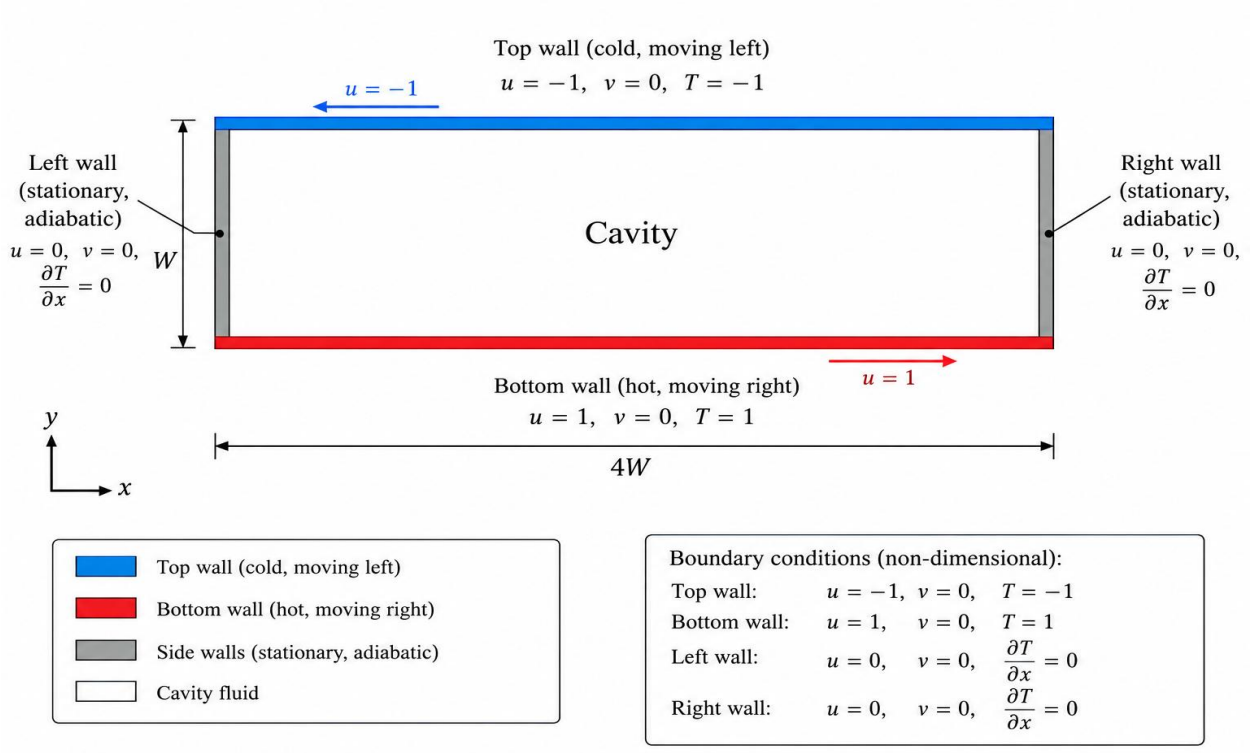


Figure 1. Rectangle cavity with hydraulics and thermal boundary conditions.

2.2. Governing Equations and Nanofluid Properties

The flow is modeled using the conservation equations of mass, momentum, and energy for an incompressible nanofluid. The governing equations are expressed in dimensionless conservative form as [17]

$$\frac{\partial Q}{\partial t} + \frac{\partial F}{\partial x} + \frac{\partial G}{\partial y} = \frac{\partial R}{\partial x} + \frac{\partial S}{\partial y} + H \tag{1}$$

$$\mathrm{Z}=\begin{bmatrix} p \\ u \\ v \\ T \end{bmatrix}, \quad F=\begin{bmatrix} u \\ p+u^2 \\ uv \\ (T-Ec\ p)u \end{bmatrix}, \quad G=\begin{bmatrix} v \\ uv \\ p+v^2 \\ (T-Ec\ p)v \end{bmatrix}, \quad R=\frac{1}{\mathrm{Re}}\begin{bmatrix} 0 \\ \dfrac{\partial u}{\partial x} \\ \dfrac{\partial v}{\partial x} \\ \dfrac{1}{\mathrm{Pr}}\dfrac{\partial T}{\partial x} \end{bmatrix},$$

$$S=\frac{1}{\mathrm{Re}}\begin{bmatrix} 0 \\ \dfrac{\partial u}{\partial y} \\ \dfrac{\partial v}{\partial y} \\ \dfrac{1}{\mathrm{Pr}}\dfrac{\partial T}{\partial y} \end{bmatrix}, \quad H=\begin{bmatrix} 0 \\ 0 \\ \dfrac{Gr}{\mathrm{Re}^2}T \\ \dfrac{Ec}{\mathrm{Re}}\Phi \end{bmatrix}, \quad \Phi=\left(\frac{\partial u}{\partial y}+\frac{\partial v}{\partial x}\right)^2+2\left(\left(\frac{\partial u}{\partial x}\right)^2+\left(\frac{\partial v}{\partial y}\right)^2\right),$$

where Q is the vector of conservative variables, F and G are the inviscid flux vectors, R and S are the viscous and thermal diffusion flux vectors, and H represents the source terms.

where Φ represents the dimensionless viscous-dissipation function. The Eckert number, (Ec), characterizes the relative importance of viscous dissipation in the energy equation. Consequently, changing (Ec) enables the contribution of viscous heating to the thermal field to be investigated.

The thermophysical properties of the water–TiO_2 nanofluid are evaluated using the mixture relations adopted in the present formulation. The effective density, dynamic viscosity, volumetric heat capacity, thermal conductivity, and thermal expansion coefficient are expressed relative to the corresponding properties of the base fluid as [18]

$$\begin{aligned} &\frac{\rho_{nf}}{\rho_{bf}}=1-C+C\frac{\rho_p}{\rho_{bf}}; \quad \frac{\mu_{nf}}{\mu_{bf}}=1+CNv; \quad \frac{\left(\rho C_p\right)_{nf}}{\left(\rho C_p\right)_{bf}}=1-C+C\frac{\left(\rho C_p\right)_p}{\left(\rho C_p\right)_{bf}}; \\ &\frac{k_{nf}}{k_{bf}}=1+CNc; \quad \frac{\beta_{nf}}{\beta_{bf}}=\frac{\rho_{nf}}{\rho_{bf}}\left[(1-C)+C\frac{(\rho\beta)_p}{(\rho\beta)_{bf}}\right]. \end{aligned} \tag{2}$$

Here, the subscripts (nf), (f), and (p) refer to the nanofluid, base fluid, and nanoparticles, respectively. The symbols (ρ), (μ), (Cp), (k), and (β) denote density, dynamic viscosity, specific heat capacity, thermal conductivity, and thermal expansion coefficient, respectively. The parameters (N_v) and (N_k) are the viscosity and thermal-conductivity model parameters used in the adopted property relations.

These effective properties are used to account for the presence of nanoparticles in the transport equations. The nanoparticle concentration is kept constant throughout the simulations so that the influence of the Eckert number can be evaluated independently of changes in particle loading.

2.3. Numerical Method and Convergence Assessment

The governing equations are discretized using the finite volume method (FVM). In this approach, the conservation equations are integrated over the computational control volumes, and the resulting fluxes are evaluated at the control-volume faces. This formulation ensures that the conservation properties of the governing equations are retained at the discrete level.

The temporal derivatives are discretized using the first-order forward Euler method. The convective and viscous terms are evaluated using the averaging procedure adopted in the numerical scheme. The resulting algebraic equations are advanced iteratively until a steady solution is obtained.

To examine the influence of viscous dissipation, simulations are performed for different Eckert numbers while keeping (Re=49), (Gr=16), (Pr=6), and (C=0.03) unchanged. Convergence histories are recorded for the selected Eckert numbers to assess the iterative behavior and the stability of the numerical solutions. The convergence criterion and the residual definition are specified consistently for all cases.

The convergence assessment is followed by a grid-independence study to determine an appropriate computational mesh. Several successively refined grids are considered, and representative quantities, including the velocity and temperature fields, are compared between the grids. The final mesh is selected when further refinement produces negligible changes in the quantities of interest. This procedure minimizes the influence of spatial discretization on the reported results while avoiding unnecessary computational expense.

The convergence behavior of the numerical simulations was examined for four Eckert numbers, namely (Ec=0.0), (0.1), (0.2), and (0.3), while maintaining the other dimensionless parameters at (Re=49), (Gr=16), and (Pr=6). Figure 2 presents the convergence histories for the different Eckert numbers. The vertical axis is plotted on a logarithmic scale to clearly illustrate the reduction in the numerical error over successive iterations.

As shown in Figure. 2, the convergence histories exhibit similar overall trends for all four Eckert numbers, indicating that varying the Eckert number within the investigated range does not produce a significant change in the convergence behavior of the numerical solution. The numerical error decreases progressively with increasing iteration number, although small fluctuations are observed

during the later stages of the iterative process. For all cases, the prescribed convergence criterion of an error below (10^{-5}) is satisfied within 1196 iterations. These results demonstrate consistent convergence behavior across the investigated Eckert numbers and provide a basis for the subsequent grid-independence study. To evaluate the influence of grid resolution on the numerical results, a grid-independence study was conducted using four computational meshes containing 6,400, 19,600, 40,000, and 90,000 control volumes. Figure 3 compares the temperature profiles obtained using these meshes along the horizontal direction of the cavity.

As shown in Figure. 3, noticeable differences are observed between the temperature profiles obtained using the coarsest mesh and those obtained using the finer meshes, particularly near the cavity walls. The results obtained with 40,000 and 90,000 control volumes exhibit substantially better agreement over most of the computational domain, indicating that the solution becomes less sensitive to further mesh refinement. Nevertheless, some differences remain near the right wall, where the temperature profile changes more sharply. Considering the overall agreement between the two finest meshes and the computational cost associated with further refinement, the mesh containing 40,000 control volumes was selected for the subsequent simulations. To quantify the grid sensitivity, the temperature profiles obtained with the two finest meshes (40,000 and 90,000 control volumes) were compared along the horizontal centerline of the cavity. The maximum local relative difference between these two meshes was approximately **3%**, while the average relative difference over the centerline was approximately **1.5%**. These differences are small and are confined primarily to the near-wall regions, where the temperature gradient is steepest. Considering this quantitative agreement and the substantially higher computational cost associated with the 90,000-cell mesh, the mesh containing 40,000 control volumes was selected for all subsequent simulations.

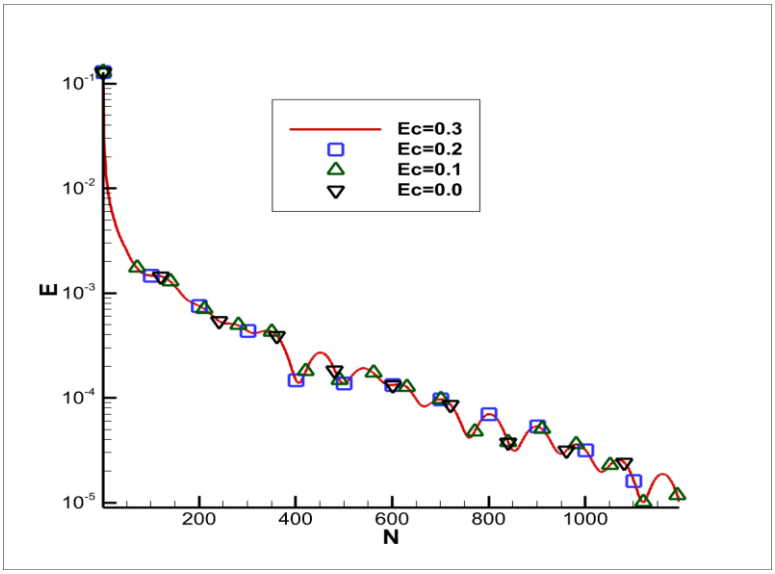


Figure 2. Convergence histories for different Eckert numbers ((Ec=0.0), (0.1), (0.2), and (0.3)).

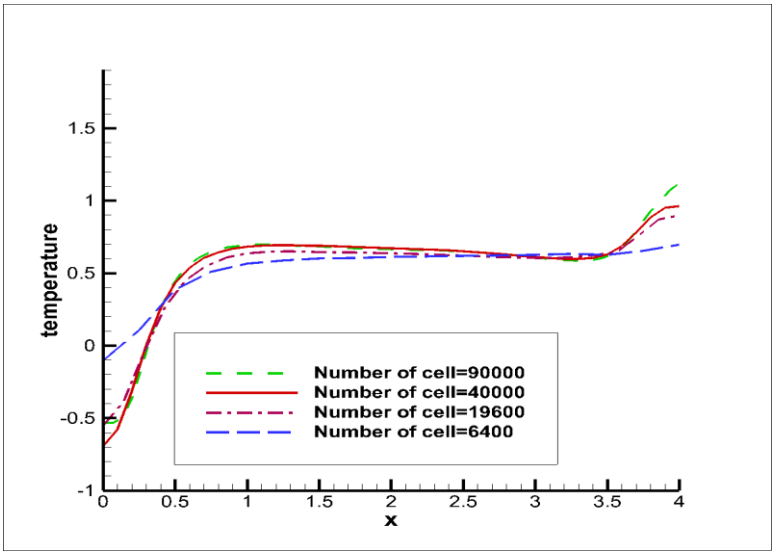


Figure 3. Grid-independence study based on the horizontal temperature profile for different numbers of control volumes.

2.4. Validation of the Numerical Model and Heat-Transfer Parameters

The numerical formulation is validated by comparing the present results with suitable reference data from previously published studies or an established benchmark problem. The comparison is performed using corresponding geometrical configurations, boundary conditions, dimensionless parameters, and physical-property assumptions. Where applicable, representative velocity and temperature profiles or integral heat-transfer quantities are used to evaluate the agreement between the present calculations and the reference results.

The validation case is selected to ensure that the comparison is physically meaningful and that differences in the governing equations or numerical assumptions do not compromise the assessment. Quantitative deviations are evaluated using an appropriate error measure, and the results are discussed before proceeding to the analysis of the flow and thermal fields.

To validate the numerical model, the skin-friction coefficient obtained in the present study was compared with the results reported by Adibi et al. [13] for Richardson numbers of Ri = 0.1, 1.0, and 10.0. The validation case corresponds to a square lid-driven cavity filled with a TiO_2–water nanofluid. The top wall moves to the right, while the bottom wall and both vertical sidewalls are stationary. Thermally, the top wall is hot, the bottom wall is cold, and the vertical sidewalls are adiabatic. The comparison was performed under otherwise identical geometrical, thermophysical,

and boundary conditions. As presented in Table 2, the present results are in good agreement with the reference data. The relative differences in the skin-friction coefficient are approximately 0.46%, 0.43%, and 0.83% for (Ri=0.1), (1.0), and (10.0), respectively. The maximum relative difference is less than 1%, indicating good agreement between the two sets of results and supporting the reliability of the present numerical formulation.

Table 2. Comparison of the skin-friction coefficient obtained in the present study with the results of Adibi et al. [13] for different Richardson numbers.

	Ri=0.1	Ri=1.0	Ri=10.0
Present work	2.20	2.31	2.39
Adibi et al.[3]	2.19	2.30	2.41

The wall shear stress and heat-transfer characteristics can be quantified using the skin-friction coefficient and the local Nusselt number. Following the definitions adopted in the present formulation, these quantities are evaluated from the wall-normal velocity and temperature gradients as [13]

$$f = \frac{2}{\mathrm{Re}} \frac{\mu_{nf}}{\mu_{bf}} \frac{\partial u}{\partial y} = \frac{2}{\mathrm{Re}} \frac{\mu_{nf}}{\mu_{bf}} \frac{u_2 - u_1}{y_2 - y_1}. \tag{3}$$

where the subscripts 1 and 2 denote adjacent computational locations used to approximate the wall-normal gradients. The signs of these quantities depend on the wall orientation and the direction of the corresponding gradients.

The numerical model, once verified for convergence and grid independence and validated against appropriate reference data, is then used to investigate the influence of the Eckert number on the flow structure and thermal transport within the cavity.

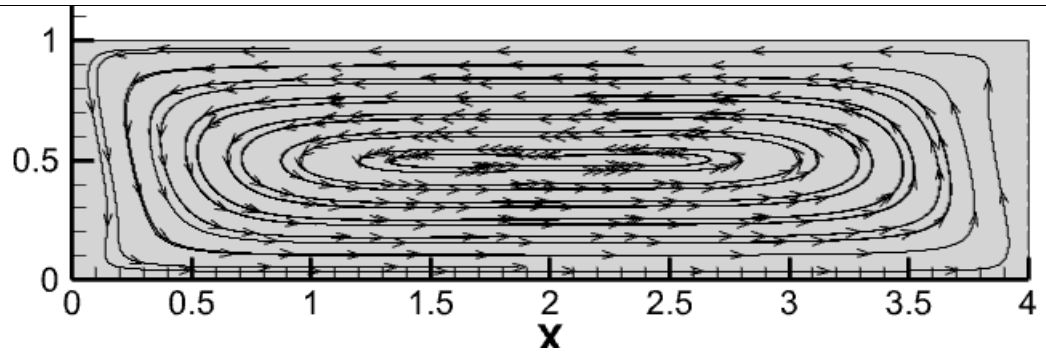
3. Results and Discussion

3.1. Flow Structure and Streamline Patterns

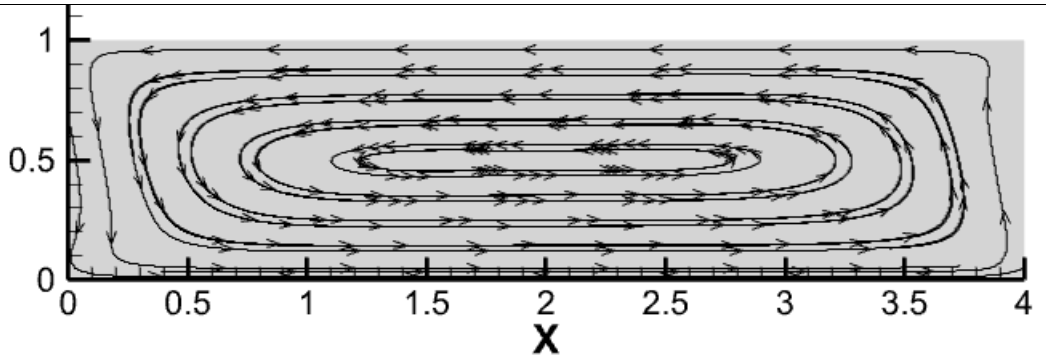
The influence of the Eckert number on the flow structure inside the rectangular cavity is investigated for (Ec=0.0), (0.1), (0.2), and (0.3), while the Reynolds, Grashof, and Prandtl numbers are maintained at (Re=49), (Gr=16), and (Pr=6), respectively. The nanoparticle volume fraction is also kept constant at (C=0.03). Figure 4 presents the streamline patterns obtained for the different Eckert numbers.

As shown in Figure. 4, the flow is characterized by a dominant recirculating region extending over most of the cavity. The overall streamline patterns remain qualitatively similar as the Eckert number increases from 0.0 to 0.3. In all cases, the flow exhibits an elongated recirculation structure consistent with the opposing motion of the upper and lower walls. No pronounced changes in the overall flow topology are apparent from the streamline distributions.

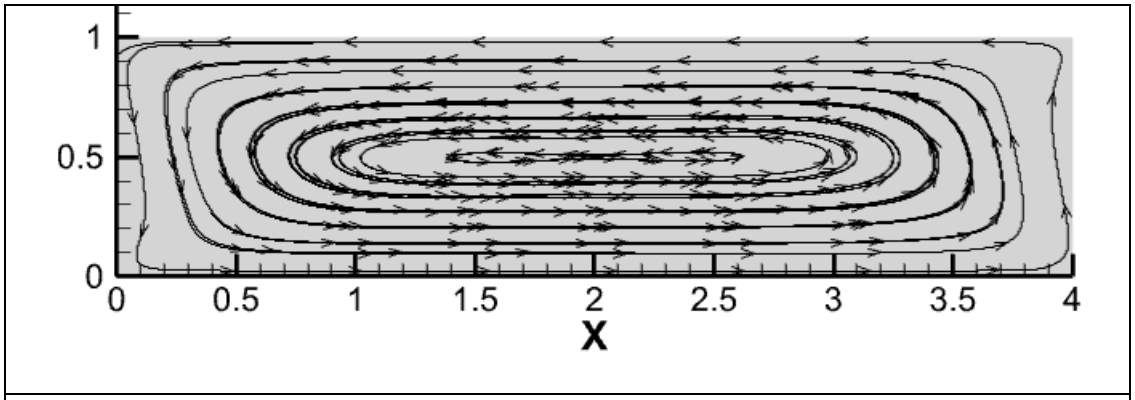
The observed similarity suggests that varying the Eckert number within the investigated range does not substantially alter the overall structure of the flow. However, streamline plots primarily illustrate the qualitative characteristics of the velocity field and may not reveal relatively small changes in velocity magnitude or local velocity gradients. Therefore, a more detailed assessment of the influence of the Eckert number requires quantitative comparisons of the horizontal and vertical velocity profiles, which are presented in the following subsection. These profiles provide a clearer basis for identifying potential differences between the simulated cases.



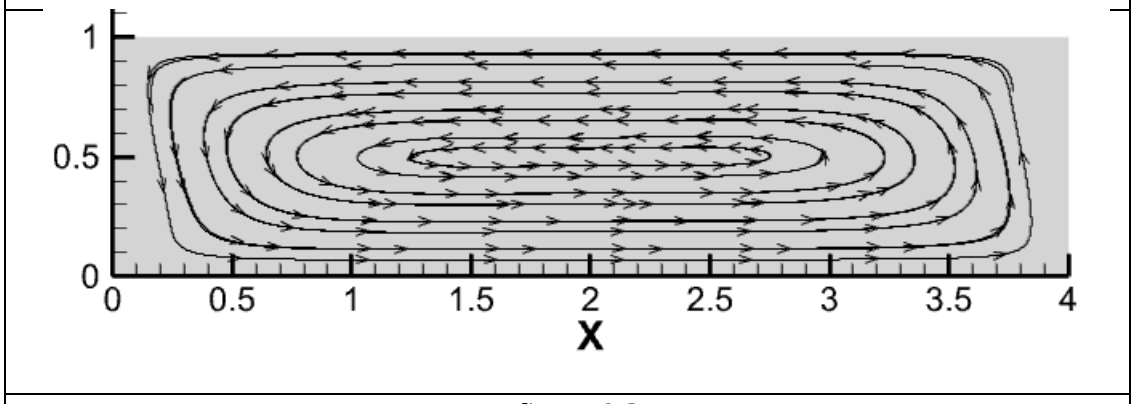
a) Ec=0.0



b) Ec=0.1



c) Ec=0.2



d) Ec=0.3

Figure 4. Streamline patterns in the cavity for different Eckert numbers: (a) (Ec=0.0), (b) (Ec=0.1), (c) (Ec=0.2), and (d) (Ec=0.3).

3.2. Velocity Profiles

The effects of the Eckert number on the velocity distribution within the cavity are investigated by comparing the horizontal and vertical velocity profiles for (Ec=0.0), (0.1), (0.2), and (0.3). The horizontal velocity component, (u), is evaluated along the vertical centerline of the cavity, whereas the vertical velocity component, (v), is examined along the horizontal centerline. The corresponding profiles are presented in Figures. 5 and 6, respectively.

Figure 5 illustrates the variation of the horizontal velocity component along the vertical centerline. The velocity changes almost linearly across a substantial portion of the cavity height, transitioning from the positive velocity imposed by the lower moving wall to the negative velocity imposed by the upper moving wall. The profiles obtained for the four Eckert numbers nearly overlap, indicating that the horizontal velocity distribution is only weakly affected by variations in the Eckert number over the range considered. Although minor differences can be observed at certain locations, no substantial change in the overall velocity profile is apparent.

The vertical velocity profiles shown in Fig. 6 exhibit a different spatial distribution. The vertical velocity remains relatively small over the central portion of the horizontal centerline, while larger variations occur closer to the sidewalls. This behavior reflects the spatial redistribution of fluid motion associated with the recirculating flow inside the cavity. Similar to the horizontal velocity component, the profiles for different Eckert numbers show a high degree of overlap over most of the domain. Some local differences are visible, particularly in regions where the vertical velocity changes more rapidly; however, the overall profile shapes remain comparable.

The close agreement between the velocity profiles indicates that increasing the Eckert number from 0.0 to 0.3 does not produce a pronounced change in the velocity field under the present operating conditions. This behavior is consistent with the similar streamline patterns discussed in Section 3.1. Since the Eckert number primarily characterizes the relative contribution of viscous dissipation to the energy equation, its influence may be more readily reflected in the temperature distribution than in the velocity field. The temperature profiles are therefore examined in the following subsection to assess the thermal response to variations in the Eckert number.

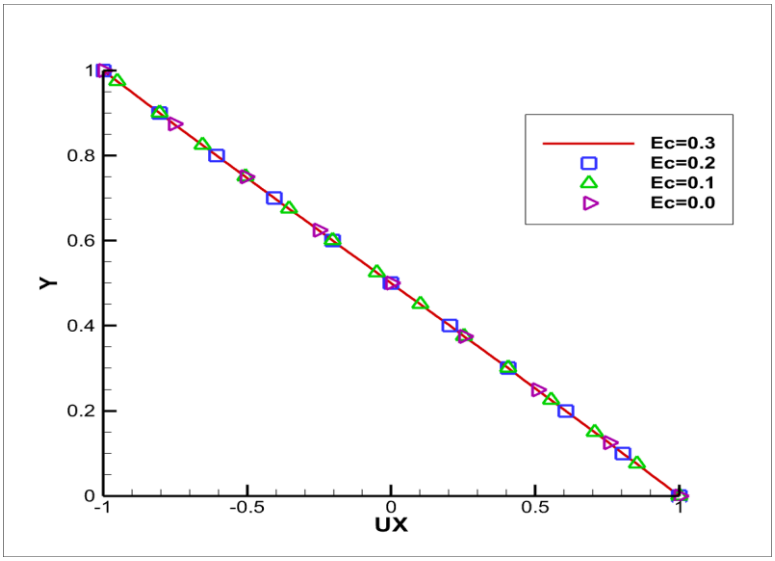


Figure 5. Horizontal velocity profiles along the vertical centerline of the cavity for different Eckert numbers.

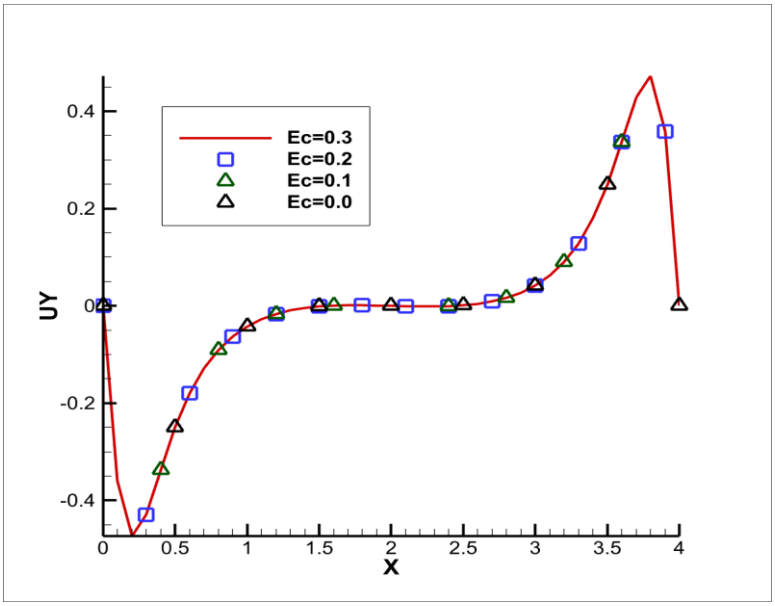


Figure 6. Vertical velocity profiles along the horizontal centerline of the cavity for different Eckert numbers.

3.3. Temperature Profiles

The effect of the Eckert number on the temperature distribution inside the cavity is investigated by comparing the horizontal and vertical temperature profiles for (Ec=0.0), (0.1), (0.2), and (0.3). The corresponding results are presented in Figs. 7 and 8. In contrast to the velocity profiles discussed in Section 3.2, the temperature distributions exhibit clear differences as the Eckert number increases, highlighting the influence of viscous dissipation on the thermal field.

Figure 7 shows the horizontal temperature profiles along the horizontal direction of the cavity. A substantial increase in temperature is observed as the Eckert number increases from 0.0 to 0.3. Over a considerable portion of the cavity, the temperature profiles follow a relatively flat trend after the initial rise near the left wall. However, the temperature level in this region increases consistently with the Eckert number. For example, the (Ec=0.3) curve remains above the profiles corresponding to the lower Eckert numbers over most of the domain. Near the right wall, the temperature increases sharply for all cases, although the magnitude of this increase depends on the Eckert number. These results indicate that viscous dissipation significantly affects the horizontal temperature distribution, particularly near the boundaries and in regions where strong temperature gradients develop.

Figure 8 presents the vertical temperature profiles along the vertical direction of the cavity. The temperature varies from the prescribed hot-wall value at the bottom to the prescribed cold-wall value at the top. The profiles exhibit a nonuniform variation across the cavity height, with a relatively broad region of gradual temperature change in the central portion and more pronounced variations

near the horizontal walls. As the Eckert number increases, the profiles shift toward higher dimensionless temperatures over most of the cavity height. The largest differences between the cases are observed in the interior region, where the temperature at (Ec=0.3) is generally higher than that at (Ec=0.2), (0.1), and (0.0).

The temperature profiles demonstrate that the Eckert number has a considerably stronger influence on the thermal field than on the overall velocity distribution under the present operating conditions. This behavior is consistent with the role of the Eckert number in quantifying the relative importance of viscous dissipation in the energy equation. As (Ec) increases, the contribution of viscous heating becomes more significant, resulting in higher temperatures within substantial portions of the cavity. Meanwhile, the prescribed temperatures at the hot and cold walls remain unchanged, and the differences between the profiles are primarily observed within the cavity interior. Overall, these results show that viscous dissipation is an important factor in determining the temperature distribution in the present lid-driven mixed-convection configuration.

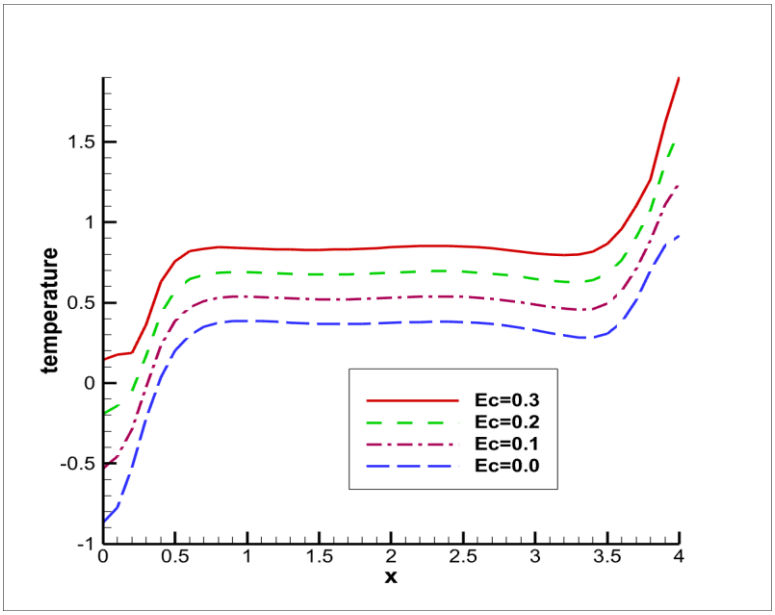


Figure 7. Horizontal temperature profiles along the horizontal centerline of the cavity for different Eckert numbers.

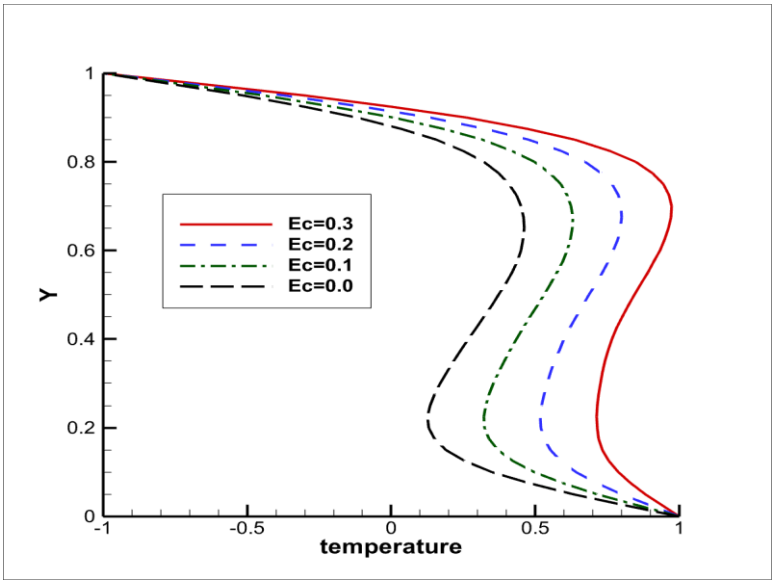


Figure 8. Vertical temperature profiles along the vertical centerline of the cavity for different Eckert numbers.

The results presented in the preceding sections demonstrate that the Eckert number affects the thermal field more noticeably than the velocity distribution in the present mixed-convection problem. Although the streamline patterns and velocity profiles remain broadly similar for (Ec=0.0), (0.1), (0.2), and (0.3), the temperature profiles exhibit clear changes with increasing Eckert number.

The weak sensitivity of the velocity field suggests that the opposing motion of the horizontal walls remains the dominant factor governing the overall flow structure under the selected operating conditions. In contrast, the systematic upward shift of the temperature profiles over much of the cavity indicates that viscous dissipation plays an important role in the energy balance. The effect is particularly apparent in regions where the temperature varies rapidly near the cavity boundaries.

These observations highlight the distinction between the mechanisms governing momentum and energy transport in the present configuration. While the overall circulation pattern is relatively insensitive to the Eckert number over the investigated range, the thermal response is considerably more sensitive to changes in viscous dissipation. Consequently, accounting for viscous heating is important when predicting the temperature distribution in lid-driven cavities containing water-based $TiO_۲$ nanofluids, even when the corresponding changes in the velocity field are relatively small.

4. Conclusions

The present study numerically investigated mixed convection in a rectangular cavity filled with a water-based (TiO_2) nanofluid at a nanoparticle volume fraction of 0.03. The cavity had an aspect

ratio of (L/H=4), with the upper and lower walls moving in opposite directions at equal dimensionless velocities. The effects of viscous dissipation were examined by varying the Eckert number from 0.0 to 0.3 while keeping the Reynolds, Grashof, and Prandtl numbers at 49, 16, and 6, respectively. The governing equations were solved using the finite volume method, and the numerical results were examined through convergence assessment, a grid-independence study, and comparison with previously published skin-friction data.

The main conclusions of this investigation can be summarized as follows:

1. **Flow structure:** The streamline patterns remain qualitatively similar for all investigated Eckert numbers. No substantial change in the overall recirculation structure is observed within the considered range.

2. **Horizontal velocity:** The horizontal velocity profile along the vertical centerline exhibits an approximately linear variation over a substantial portion of the cavity height. The profiles for different Eckert numbers nearly overlap, indicating a limited influence of viscous dissipation on this velocity component.

3. **Vertical velocity:** The vertical velocity profile along the horizontal centerline exhibits larger variations near the sidewalls and relatively small values over much of the central region. Despite these spatial variations, the overall profiles remain broadly similar for the different Eckert numbers.

4. **Temperature distribution:** Unlike the velocity field, the temperature distribution is clearly affected by the Eckert number. Increasing (Ec) generally raises the dimensionless temperature over a substantial portion of the cavity, demonstrating the importance of viscous dissipation in the thermal energy balance.

5. **Relative sensitivity of the flow and thermal fields:** Under the present conditions, the influence of the Eckert number is more pronounced in the temperature field than in the overall velocity distribution. This finding emphasizes the need to account for viscous dissipation when analyzing heat transfer in moving-wall cavities, even when the overall flow structure changes only slightly.

Overall, the results indicate that viscous dissipation primarily modifies the thermal response of the water-TiO_2 nanofluid, whereas the main features of the flow remain relatively stable over the investigated Eckert-number range. These findings provide insight into the coupled momentum and energy transport processes in lid-driven cavities and clarify the role of viscous heating under the

selected mixed-convection conditions. The present results are obtained for Re = 49 and Gr = 16 (Ri ≈ 0.0067). At higher Reynolds and Grashof numbers, the flow may become unsteady and the relative importance of viscous dissipation may change; therefore, the quantitative conclusions reported here should be extrapolated with caution. Nevertheless, the qualitative finding that viscous dissipation affects the thermal field more strongly than the velocity field is expected to remain valid in forced-convection-dominated regimes. Although the present validation is based on the skin-friction coefficient and on the physical consistency of the thermal field, a dedicated validation of the temperature profile or Nusselt number against a benchmark viscous-dissipation case would further strengthen the thermal predictions and is recommended for future work."

References

[1] U. Ghia, K. N. Ghia, and C. T. Shin, "High-Re solutions for incompressible flow using the Navier–Stokes equations and a multigrid method," Journal of Computational Physics, vol. 48, no. 3, pp. 387–411, 1982.

[2] R. Iwatsu, J. M. Hyun, and K. Kuwahara, "Mixed convection in a driven cavity with a stable vertical temperature gradient," International Journal of Heat and Mass Transfer, vol. 36, no. 6, pp. 1601–1608, 1993.

[3] S. U. S. Choi and J. A. Eastman, "Enhancing thermal conductivity of fluids with nanoparticles," in Proceedings of the ASME International Mechanical Engineering Congress and Exposition, San Francisco, CA, USA, 1995, pp. 99–105.

[4] A. J. Chamkha and E. Abu-Nada, "Mixed convection flow in single- and double-lid driven square cavities filled with water–Al_2O_3 nanofluid: Effect of viscosity models," European Journal of Mechanics—B/Fluids, vol. 36, pp. 82–96, 2012.

[5] M. Alinia, D. D. Ganji, and M. Gorji-Bandpy, "Numerical study of mixed convection in an inclined two sided lid driven cavity filled with nanofluid using two-phase mixture model," International Communications in Heat and Mass Transfer, vol. 38, no. 10, pp. 1428–1435, 2011.

[6] D. Chatterjee, S. K. Gupta, and B. Mondal, "Mixed convective transport in a lid-driven cavity containing a nanofluid and a rotating circular cylinder at the center," International Communications in Heat and Mass Transfer, vol. 56, pp. 71–78, 2014.

[7] M. A. Sheremet and I. Pop, "Mixed convection in a lid-driven square cavity filled by a nanofluid: Buongiorno's mathematical model," Applied Mathematics and Computation, vol. 266, pp. 792–808, 2015.

[8] A. R. Rahmati, A. Rayat Roknabadi, and M. Abbaszadeh, "Numerical simulation of mixed convection heat transfer of nanofluid in a double lid-driven cavity using lattice Boltzmann method," Alexandria Engineering Journal, vol. 55, no. 4, pp. 3101–3114, 2016.

[9] R. Jmai, B. Ben-Beya, and T. Lili, "Numerical analysis of mixed convection at various walls speed ratios in two-sided lid-driven cavity partially heated and filled with nanofluid," Journal of Molecular Liquids, vol. 221, pp. 691–713, 2016.

[10] M. Hemmat Esfe, S. Saedodin, E. Hasani Malekshah, A. Babaie, and H. Rostamian, “Mixed convection inside lid-driven cavities filled with nanofluids,” Journal of Thermal Analysis and Calorimetry, vol. 135, pp. 813–859, 2019.

[11] S. Izadi, T. Armaghani, R. Ghasemiasl, A. J. Chamkha, and M. Molana, “A comprehensive review on mixed convection of nanofluids in various shapes of enclosures,” Powder Technology, vol. 343, pp. 880–907, 2019.

[12] Z. Boulahia, A. Wakif, and R. Sehaqui, “Numerical study of mixed convection of the nanofluids in two-sided lid-driven square cavity with a pair of triangular heating cylinders,” Journal of Engineering, vol. 2016, Article ID 8962091, 2016.

[13] T. Adibi, S. E. Razavi, O. Adibi, M. Vajdi, and F. Sadegh Moghanlou, “The response of nano-ceramic doped fluids in heat convection models: A characteristics-based numerical approach,” Scientia Iranica, vol. 28, no. 5, pp. 2671–2683, 2021.

[14] N. Keklikcioğlu Çakmak, H. H. Durmazuçar, and K. Yapıcı, “A numerical study of mixed convection heat transfer in a lid-driven cavity using Al_2O_3-water nanofluid,” International Journal of Chemistry and Technology, vol. 4, no. 1, pp. 22–37, 2020.

[15] O. Aydın and A. Kaya, “Mixed convection of a viscous dissipating fluid about a vertical flat plate,” Applied Mathematical Modelling, vol. 31, no. 5, pp. 843–853, 2007.

[16] M. M. Khairi, et al., "Heat and mass transfer enhancement in a solar still using a photovoltaic-powered oscillating heated wall-jet inlet," *International Communications in Heat and Mass Transfer*, vol. 178, p. 111648, 2026.

[17] T. Adibi, et al., "Impact of artificial compressibility on the numerical solution of incompressible nanofluid flow," *Computers, Materials & Continua*, vol. 74, no. 3, pp. 5123–5139, 2023.